

Permafrost peatland development at thermokarst lake margins in the northern Greater Khingan Mountains of Northeast China: Rapid areal increase and carbon accumulation since the 1950s

Jiangtao Gao^{a,c}, Jinxin Cong^b, Guangxin Li^a, Yingjie Shi^{a,c}, Dongxue Han^{a,*}, Guoping Wang^a, Chuanyu Gao^{a,*}

^a State Key Laboratory of Black Soils Conservation and Utilization, Northeast Institute of Geography and Agroecology, Chinese Academy of Sciences, 130102 Changchun, China

^b School of Geographical Sciences, Changchun Normal University, 130032 Changchun, China

^c University of Chinese Academy of Sciences, 100049 Beijing, China

ARTICLE INFO

Editor: H. Falcon-Lang

Keywords:

Permafrost peatland
Thermokarst lake
Peatland initiation
Carbon accumulation
post-bomb ¹⁴C dating

ABSTRACT

Peatlands are major carbon sinks and play a crucial role in the carbon cycle. Permafrost peatlands in mid-to-high latitude regions are highly sensitive to climate change, leading to the formation of thermokarst lakes in widely distributed areas of permafrost degradation. In this study, seven peat cores from typical peatlands at thermokarst lake margins in the northern Greater Khingan Mountains of northeast China were used to reconstruct the formation age and accumulation history of peatlands, and to analyze the change in the stability of the peatland carbon pool over time. Results show that drought events and local topography influence the lakeward expansion of the peatlands at thermokarst lake margins, with expansion rates ranging from 2 cm yr⁻¹ to 32 cm yr⁻¹. Strongly influenced by hydrological fluctuations and warming, the carbon accumulation of the studied peatlands commenced with a stage of slow accumulation, and then entered a rapid accumulation stage after the 1950s, with the carbon accumulation rates increasing from $45.2 \pm 5.5 \text{ g C m}^{-2} \text{ yr}^{-1}$ to $330.5 \pm 14.4 \text{ g C m}^{-2} \text{ yr}^{-1}$. Moreover, the stability of the peatland carbon pool has improved with more stable aromatic compounds increasing from 29.3 % to 32.3 %, as peat accumulation has entered a rapid accumulation stage.

1. Introduction

Peatlands, with their significant carbon storage capacity, play a crucial role as carbon sinks. They cover an estimated 340 million hectares worldwide and store 600 Pg C (Tarnocai et al., 2009; Yu, 2011). Despite occupying only 3–4 % of the global land area, boreal peatlands have accumulated nearly 30 % of the global soil carbon stock throughout the Holocene (Gorham, 1991). More than half of the boreal peatlands are widely distributed in permafrost regions (continuous, discontinuous and isolated) of mid-to-high latitude areas, along with abundant ponds and lakes (Olefeldt et al., 2021). The impermeability and cooling effect of underlying permafrost create a cold and moist environment for peat accumulation (Yu et al., 2010; Swindles et al., 2015). Peatlands accumulate approximately 100 Tg of organic carbon annually, equivalent to 370 Tg of CO₂ sequestered in the peatlands carbon pool (Strack, 2008), making peatlands the most efficient natural

ecosystem for long-term carbon sequestration (Page and Baird, 2016; Temmink et al., 2022). Thus, understanding the formation and carbon accumulation process of peatlands is essential for analyzing the carbon balance in permafrost region.

Peatland formation is driven by a range of complex processes, with the aquatic-terrestrial transition being a key mechanism. Lake terrestrialization, a lacustrine ecosystem senescence, typically initiates in shallow and freshwater basin with moderate water fluctuations (Chai, 1990). The permafrost regions of the Northern Hemisphere are particularly vulnerable to global climate warming (Schuur et al., 2015; Swindles et al., 2015). Warming accelerates the thawing of ice-rich permafrost, leading to land subsidence and the creation of unique landforms such as thermokarst lakes (Sannel and Kuhry, 2011; Vonk et al., 2015; Olefeldt et al., 2016). Variations in local topography of lake basin play crucial roles in the initiation of peatlands, the peat-forming plants initiate growth at locations with more favorable conditions

* Corresponding authors.

E-mail addresses: handongxue@iga.ac.cn (D. Han), gaochuanyu@iga.ac.cn (C. Gao).

(Juselius-Rajamäki et al., 2023). Over thousands of years, plant remains from algal mats to floating and emergent plants gradually accumulate, filling the lake and forming peatlands (Payette et al., 2004; Ruppel et al., 2013). While surface of peatland rise, hydrological changes also lead to the succession of aquatic to terrestrial plants and a shift from minerotrophic peatlands have a warming effect to ombrotrophic peatlands are considerable net sinks for atmospheric carbon (Hugelius et al., 2020; Juselius-Rajamäki et al., 2025). Changes in supply types and dominant plant species may lead to differences in the litter composition and carbon accumulation rates (Breeuwer et al., 2009; Olid et al., 2017). The composition of organic matter in litter also impacts the stability of peat organic carbon (Hutchings et al., 2019; Cong et al., 2020). The stability of peat organic carbon ultimately determines the role and function of the peatlands carbon pool in future carbon sink systems.

Lake terrestrialization is significantly influenced by external conditions, particularly drought events and global warming (Kratz and Dewitt, 1986; Ireland et al., 2013; Zhang et al., 2019). The timing and rate of lake water table changes strongly affected by drier climate (e.g. Williams et al., 2010; Ireland et al., 2013). Then the water table changes and global warming might accelerate the plants succession and enhance the net primary productivity (NPP) of plants (Breeuwer et al., 2009; Ireland et al., 2013; Juselius-Rajamäki et al., 2025). Additionally, the channels formed by permafrost thaw may establish a close connection between lakes and surrounding water systems, thereby affecting the hydrological conditions of thermokarst lake (Olefeldt et al., 2021). All external conditions might accelerate the infilling process of peatland and terrestrialization, resulting in the former lake region transforms from a net carbon source to a peatlands ecosystem with a strong carbon sink capacity on shorter timescales (Ruppel et al., 2013; Juselius-Rajamäki, 2025).

Compared to other lake types, thermokarst lake shores support more hydrophilic *Sphagnum* and sedges rapidly growing, with shallow basin providing favorable conditions for peatlands formation (Olefeldt et al., 2016; Olefeldt et al., 2021; Shaposhnikova et al., 2023). Then peatlands go through autogenic succession with peat accumulation where after about 100 years the peat surface is rapidly raised above the water table and dominated by dry-adapted *Sphagnum* and shrubs (Camill, 1999; Olefeldt et al., 2021). Although many studies have established the relationship between permafrost peatlands carbon balance and environmental changes (Roulet et al., 2007; Heffernan et al., 2020; Harris et al., 2023), the process of peatlands formation along climate-driven thermokarst lake margins and its impact on regional carbon budgets remains unclear.

The Greater Khingan Mountains, located at the southernmost edge of the subarctic and mid-high latitude permafrost regions, are experiencing more intense climate warming than other areas (Liu et al., 2007). In recent years, climate change has caused the southern boundary of permafrost distribution in this region to shift northward by more than 100 km, resulting in permafrost degradation and significant surface subsidence in part areas (Zhou et al., 2000). With continued climate warming expected over the next few decades (Salinger, 2005), this will have a strong impact on peat accumulation and the stability of carbon pool at thermokarst lake margins of the Greater Khingan Mountains. Therefore, we collected seven peat cores from peatlands at thermokarst lake margins in the northern permafrost region of the Greater Khingan Mountains, conducted AMS ^{14}C dating, FTIR spectroscopy, and physical indicators such as dry bulk density and organic matter content of peat. We aimed 1) to reconstruct the infilling process of peatlands, 2) to quantify the carbon accumulation rates and estimate carbon stock increments in peatlands, and 3) to analyze the change in the stability of the peatland carbon pool over time at thermokarst lake margins.

2. Materials and methods

2.1. Study area

The study area is located within the permafrost zone of the northern Greater Khingan Mountains in Northeast China ($52^{\circ}55'\text{N}$, $122^{\circ}45'\text{E}$) (Fig. 1a), the elevation ranges from 451 to 477 m (Fig. 1b). The average annual temperature is -4.5°C , with the highest mean temperature of 17.6°C in July. Annual precipitation is 550 mm, with the highest monthly rainfall occurring in July, averaging 117.1 mm. Snow depth averages 14 cm from November to March over the past five years. The thermokarst lake is roughly elliptical and isolated, with no drainage channels or water networks observed around the lake. And the thermokarst lake with a long axis measuring about 240 m (northwest to southeast) and a short axis measuring about 110 m (northeast to southwest), covering an area of $21,000\text{ m}^2$. The lake's deepest point reaches 2–3 m, while the water table depth in surrounding peatlands from 10 to 30 cm. Surrounding peatlands exhibit a heterogeneous landscape of plant communities radiating from the lake center, including a sedge-dominated peatland community (*Typha* and *Equisetum*), a shrub-dominated peatland community (*Vaccinium uliginosum*, *Chamaedaphne calyculata*, and *Sphagnum*), and a forested peatland community (*Betula pendula* and *Larix gmelinii*).

2.2. Fieldwork sampling

In August 2023, seven peat cores were collected along two transects surrounding a thermokarst lake (Fig. 1b), both of which exhibited similar plant gradients. At each plant succession zone, complete peat cores were collected from the surface to the basal sediments, using Russian peat corer and sharp shovel. Transect N included three cores: N3 (shrub and *Sphagnum* -dominated zone), N2 (sedge-shrub transition zone), and N1 (sedge-dominated zone). Transect S included four cores: S1 (sedge-dominated zone), S2 (sedge-shrub transition zone), S3 (shrub and *Sphagnum*-dominated zone), and S4 (forest-shrub transition zone). To minimize structural compression, all cores were immediately sectioned at 1 cm intervals in situ.

2.3. Chronology and peat properties

The organic matter of 22 peat samples in collected peat cores were dated using accelerator mass spectroscopy (AMS) ^{14}C radiocarbon dating in the State Key Laboratory of Loess and Quaternary Geology, Institute of Earth Environment, Chinese Academy of Sciences. Pre-bomb and post-bomb ^{14}C dates were calibrated to calendar ages with IntCal 20 (Reimer et al., 2020) and Bomb 21 NHZ1 datasets on CALIBomb [WWW program] (<http://calib.org>). Finally, calibrated ages were rounded to the nearest 5 years. The fresh samples were weighed in aluminum tins with a fixed volume and dried in an oven at 105°C for 24 h to determine the sample weight and calculate the moisture content, which allowed for the determination of dry bulk density (DBD). After drying, the samples were placed in an agate mortar, ground to pass through a 100-mesh sieve (0.15 mm), and the organic carbon content (C-C) was measured. The organic matter content (OM) was calculated by multiplying the C-C by a factor of 1.724 (Silvestri et al., 2019), and the total nitrogen (TN) in the peat was measured by Kjeldahl method (Yao et al., 2022).

2.4. FTIR spectroscopy

Fourier transform infrared spectroscopy (FTIR) was employed to determine the abundance of major polysaccharide functional groups. The 2 mg dried samples and 200 mg dried KBr were mixed to a KBr pellet. The FTIR spectrum of the peat samples was then obtained using an FTIR spectrometer. The measurement were recorded from 4000 to 400 cm^{-1} , with a resolution of 2 cm^{-1} . Each sample was scanned 32 times and the average spectrum was recorded. Absorption peaks were

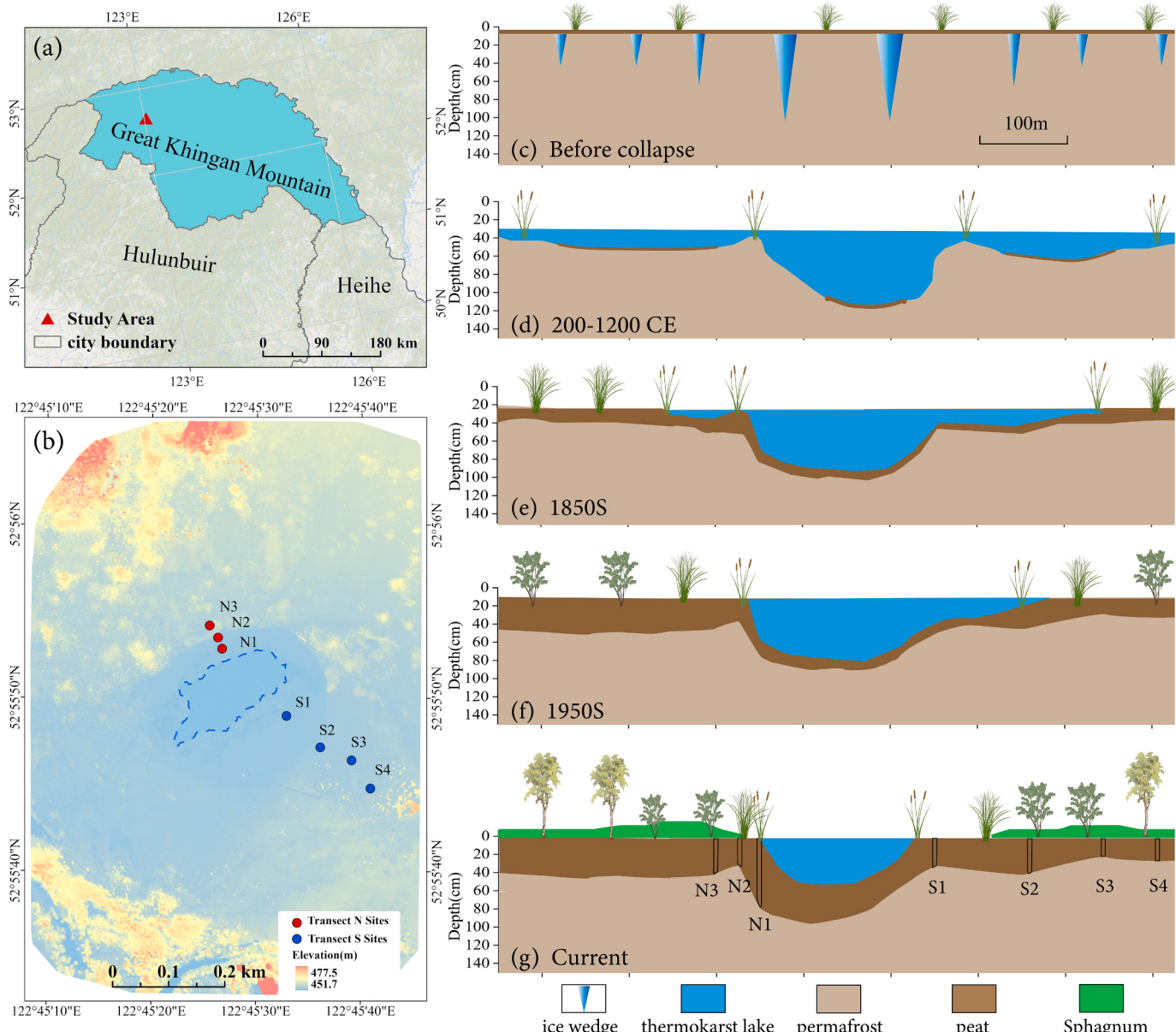


Fig. 1. (a) (b) Location of sites in the Greater Khingan Mountains, northeast China. Transect N includes N3-N1. Transect S includes S1-S4. (c) the original permafrost. (d) thermokarst lake forming in ice-rich or low-lying areas during warm periods, aquatic plant grows first in relatively higher regions. (e) the peatland development at the “Slow accumulation stage”. (f) the peatland development at the “Rapid accumulation stage”. (g) modern peatland features beside the thermokarst lake.

used to indicate the structural units present in the organic matter, which served as markers for the chemical composition of the peat. The contents of carbohydrate and aromatic substances in the peat were estimated based on their respective FTIR absorption peaks. The carbohydrate peak (carb) is located around 1030 cm^{-1} , while the aromatic peaks (arom15 and arom16) appear around 1510 cm^{-1} and 1630 cm^{-1} , respectively (Hodgkins et al., 2018; Cong et al., 2020).

2.5. Statistical calculation and analysis

Based on the age-depth($r\text{ cm yr}^{-1}$), DBD (g cm^{-3}) and C-C (%), the carbon accumulation rates (CARs) ($\text{g C m}^{-2}\text{ yr}^{-1}$) was calculated according to the following eq. (1) (Tolonen and Turunen, 1996):

$$\text{CARs} = r \times \text{DBD} \times \text{C.C} \times 100 \quad (1)$$

The peatlands C stock (t) was obtained for each area following the Eq. (2)(3):

$$S_i = A_i \times \text{CAR}_i \times 10^{-6} \quad (2)$$

$$\text{C stock} = \sum_{i=661}^{2023} S_i \quad (3)$$

Where $i \in (661, 2023)$. A_i = annual peatlands area (m^2), CAR_i = annual average CARs ($\text{g C m}^{-2}\text{ yr}^{-1}$), S_i = annual carbon stock increments. We hypothesize that the peatlands infilling at the lake's long axis follows a similar pattern to the transects direction (short axis), and estimated the carbon stock of peatlands from cores N3 to S4, with the total peatlands area simplified as an ellipse (exclude lake area).

The statistical analysis was conducted using SPSS 25. We applied analysis of variance (ANOVA) and Tukey's post-hoc test to the data on DBD, OM, CARs, and FTIR to analyze the differences in the physico-chemical properties of organic matter in the peat cores. We used two-tailed *t*-tests and linear regression analysis to examine the causes of changes in organic carbon stability for FTIR indices and TN in peat from

different cores and depths.

3. Results

3.1. Depositional variations

The variations observed between the sample layers reflect differences in the depositional environment. The peat layers are primarily composed of plant remains and typically appear dark brown. The sediments are generally brown, dark yellow color. In the core samples we collected, sediment layers were observed at the bottoms of cores N3, N2, and S2, which are located closer to the thermokarst lake shores. At the bottom of cores N3 (67 cm) and N2 (31 cm), dark brown and yellow fine-grained sediments are present, while at the bottom of the core S2 (44 cm), a gravelly mixed layer is observed. These variations in appearance can identify the transitional boundary between peat and lake sediments.

3.2. Initial formation and infilling of peatland

Through AMS ^{14}C dating of the peat at thermokarst lake margins in the Greater Khingan Mountains reveals that the oldest basal age of the peat layers ($\text{OM} \geq 30\%$) near the thermokarst lake dates back to 660 CE, while the youngest peat basal age is 1960 CE. Specifically, peat formation began at site core N2 (30 cm-660 CE), and then core S2 (43 cm-1340 CE), core N1 (80 cm-1650 CE), core S1 (30 cm-1710 CE), core S4 (25 cm-1710 CE), and the latest at core N3 (66 cm-1955 CE) and S3 (50 cm-1960 CE). The detailed information was shown in Table 1 and Table S2. The infilling process of peatlands were divided into three stages of lakeward expansion. The first stage that the earliest peat accumulation in core N2, with expansion towards cores N3 and N1, at rates of 2 cm yr^{-1} . The second stage that peat accumulation began earlier in core S2, and then expansion towards cores S1 and S4, at rates of 22 cm yr^{-1} and 32 cm yr^{-1} . The third stage involved expansion towards the lake center from cores N1 and S1, with expansion rates of approximately 4 cm yr^{-1} and 21 cm yr^{-1} , respectively.

3.3. Physicochemical characteristics

Here, the physicochemical indicators include dry bulk density (DBD), organic matter content (OM), and total nitrogen (TN), which can

Table 1
Calibrated Accelerator Mass Spectrometry (AMS) radiocarbon dates of peat cores.

Lab no.	Core-Depth (cm)	AMS ^{14}C age (^{14}C yr BP)	elected cal. Age range (1σ) (cal. yr CE)	Cal. age used in this study (cal. yr CE)
XA60651	N3-30	modern	2010–2012	2010
XA60652	N3-45	modern	2001–2002	2000
XA60653	N3-66	modern	1956–1957	1955
XA60616	N2-10	modern	1994–1995	1995
XA60617	N2-20	23 ± 13	1954–1955	1955
XA60618	N2-30	1356 ± 16	647–675	660
XA60611	N1-30	modern	2010–2012	2010
XA60612	N1-45	modern	1989–1990	1990
XA60613	N1-60	modern	1957	1957
XA60614	N1-70	0 ± 13	1954–1955	1955
XA60615	N1-80	253 ± 14	1639–1663	1650
XA60668	S1-5	modern	2009–2011	2010
XA60671	S1-30	94 ± 17	1694–1725	1710
XA60656	S2-10	modern	2013–2015	2015
XA60658	S2-30	modern	2003–2004	2005
XA60659	S2-43	580 ± 18	1317–1361	1340
XA60661	S3-20	modern	2015–2017	2015
XA60662	S3-30	modern	2005–2007	2005
XA60664	S3-50	modern	1958	1960
XA60665	S4-5	modern	2018–2019	2020
XA60666	S4-15	modern	1956–1957	1955
XA60667	S4-25	47 ± 16	1701–1720	1710

help us better distinguish the interface between sediment and peat. In all core samples, the DBD increases with depth. The mean DBD of the lower peat layer (ranging from 0.10 to 0.18 g cm^{-3}) is significantly higher than the upper peat layer (ranging from 0.06 to 0.11 g cm^{-3}) (Table S1). In contrast, the OM in the peat layer decreases with depth (Figs. 2–3). There are significant differences in the indicators between thermokarst lake sediments and peat layers, which provide evidence for distinguishing the boundary between lake sediment and peat. Specifically, at the bottom of cores N3, N2, and S2, there are clear abrupt changes in both DBD and OM. In core N3, at 66 cm, DBD is 0.09 g cm^{-3} and OM is 69.3 %, while at 67 cm, DBD increases to 0.6 g cm^{-3} and OM decreases to 24.7 %. In core N2, at 30 cm, DBD is 0.17 g cm^{-3} and OM is 62.4 %, while at 31 cm, DBD increases to 1.1 g cm^{-3} and OM decreases to 4.5 %. In core S2, at 43 cm, DBD is 0.15 g cm^{-3} and OM is 56.8 %, while at 44 cm, DBD increases to 0.53 g cm^{-3} and OM decreases to 23.7 % (Figs. 2–3).

3.4. Carbon accumulation rates

Through the analysis of carbon accumulation rates (CARs) and corresponding ages in all cores, we observe that CARs in most peat cores initially exhibit low values (i.e. “Slow accumulation stage”), the mean range of CARs from 4.9 ± 0.1 to $127.5 \pm 10.3 \text{ g C m}^{-2} \text{ yr}^{-1}$. The peat layers with a CARs increase rate significantly higher than the average rate as shift points. A shift point is observed around 1955 CE, the CARs showed a marked increase and entered “Rapid accumulation stage” after 1955 CE, the mean range of CARs from 110.1 ± 4.7 to $475.8 \pm 61.0 \text{ g C m}^{-2} \text{ yr}^{-1}$ (Fig. 4a). From a spatiotemporal perspective, among the five peat cores (N2, N1, S1, S2 and S4) where CARs shift points were identified. As the peatlands expanded towards the center of thermokarst lake, the CARs in the distal regions of the thermokarst lake shore earlier exhibited the shift points. Within a decade from 1950 to 1960 CE, five peat cores transitioned into the “Rapid accumulation stage”. The cores S1 and S2 transitioned into the “Rapid accumulation stage” until 2010 and 2004 CE (Fig. 4a).

3.5. FTIR

The carbohydrate content ranges from 24.2 ± 0.3 to $33.3 \pm 1.0 \%$, and the aromatic content ranges from 27.0 ± 0.6 to $35.5 \pm 0.5 \%$ (Fig. 4c). The linear regression analysis of the carbohydrate and aromatic contents in the peat cores relative to the distance from each sampling site to the thermokarst lake shore showed distinct patterns. As the distance from the cores to the lake shore increased, aromatic content decreased during both stages, while carbohydrate content increased during the “Slow accumulation stage” (Fig. 4b). The linear regression analysis of the carbohydrate contents and TN contents revealed that in most peat samples with higher TN content, carbohydrate content was generally lower (Fig. S1).

4. Discussion

4.1. Areal increase of peatlands

Through the analysis of peat samples data, we have determined the lake formation age and the initiation age of peat accumulation, reconstructing the infilling process of peatlands following the fluctuations of water table. Based on the initiation age of peat layers, we hypothesize that a warm climatic period led to the permafrost thawing between 200 and 1200 CE (Fig. 5g), resulting in the formation of thermokarst lake in low-lying and ice-rich areas (Fig. 1d). After the formation of thermokarst lake, the lake sediments (plant remains and organic matter) continued to decompose and accumulate, providing nutrient conditions for the peat-forming plants.

The organic matter (OM) content and dry bulk density (DBD) values, following abrupt changes, fall below the typical upper limits for peat,

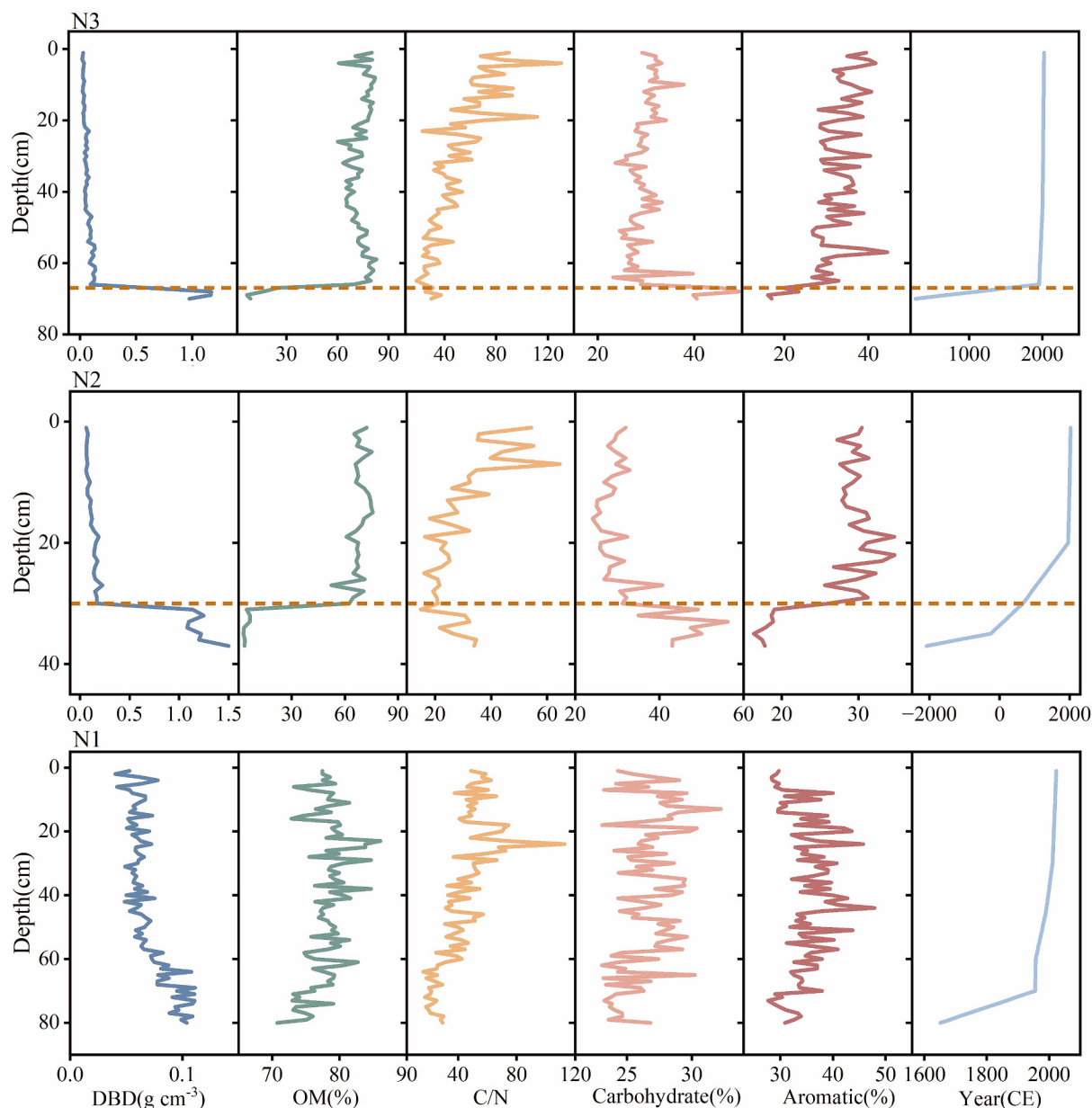


Fig. 2. The physicochemical indicators and AMS radiocarbon dates in Transect N. The dashed line represents the boundary layer between the sediment and peat in cores N1 and N2.

such as DBD = 0.3 g cm⁻³ and OM = 30 % (Morris et al., 2022). Based on these limits, we infer the contact boundary between the basal peat layers and sediments. The initiation of peatlands is typically associated with fluctuations of water table (Ruppel et al., 2013; Zhang et al., 2019). Thus, the formation ages of basal peat layers can provide insights into historical water table variations (Zhang et al., 2019). Generally, the autogenic terrestrialization is characterized by the systematic decrease of basal peat ages towards the central lake (Kratz and Dewitt, 1986). However, in this study, the peat basal ages did not follow a clear chronological sequence, suggesting that topographic variations play a significant role in controlling the infilling process of peatlands. Peat initiation occurred at multiple locations favorable for the growth of peat-forming plants and subsequently coalesce into a single, cohesive peatland (Juselius-Rajamäki et al., 2023). In higher elevation areas within the lake basin, such as cores N2 and S2, peat-forming plants colonized first, leading to earlier peat accumulation. Additionally, the study area's topography shows that the northwest (transect N) is higher, while the southeast (transect S) is lower. Consequently, the water table

in the northwest reached the threshold for plant growth earlier, resulting in earlier peat initiation in transect N compared to transect S.

The expansion of peatlands typically corresponds to or closely follows regional drought periods lasting from several decades to centuries (Ireland et al., 2013; Ruppel et al., 2013; Zhang et al., 2019). Here, the lakeward expansion of peatlands at thermokarst lake margins in the Greater Khingan Mountains corresponds to drought periods identified in paleoclimate reconstructions from northeastern China: several drought events occurred in northeastern China (Hong et al., 2001) (Fig. 5g), followed by a cold-dry period from approximately 1350 to 1650 CE, then a warmer and drier climate regime since 1650 CE (Han et al., 2019). These drought events accelerated the decline of lake water table, creating favorable conditions for plant growth and peat accumulation. Additionally, drainage channels caused by thawing of permafrost also might promote water table decline (Klein et al., 2013), but with no drainage channels or water networks we observed around the thermokarst lake. The primary factor controlling the peatland expansion were the slope of topography and severity of drought events (Campbell et al.,

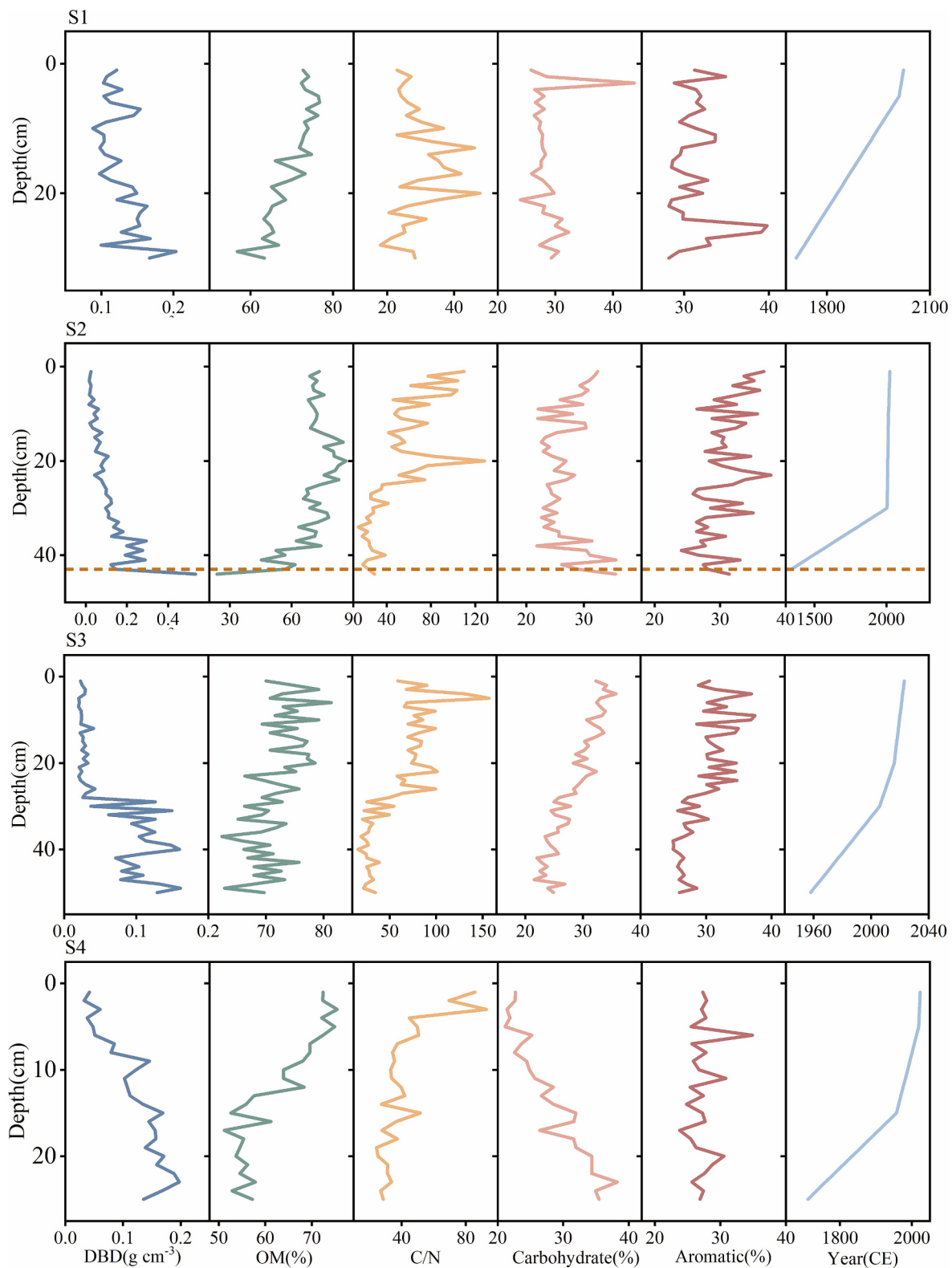


Fig. 3. The all indicators and AMS radiocarbon dates in Transect S. The dashed line represents the boundary layer between the sediment and peat in core S2.

1997; Fewster et al., 2025; Juselius-Rajamäki, 2025). Compared to the transect S, although drought events were longer time span (Fig. 5g), subsoil slopes were steeper in the transect N. As a result, the peatlands expansion rates in transect S ($21\text{--}32 \text{ cm yr}^{-1}$) is significantly higher than transect N ($2\text{--}4 \text{ cm yr}^{-1}$). As the peatland expansion close to the lake center, where the basin may be markedly steeper slow the expansion

rates. Given the current trend of areal increase, it is highly likely that the thermokarst lake will completely transform into peatlands by 2300 CE.

4.2. Peat accumulation and carbon dynamics

According to the CARs and shift points, the carbon accumulation

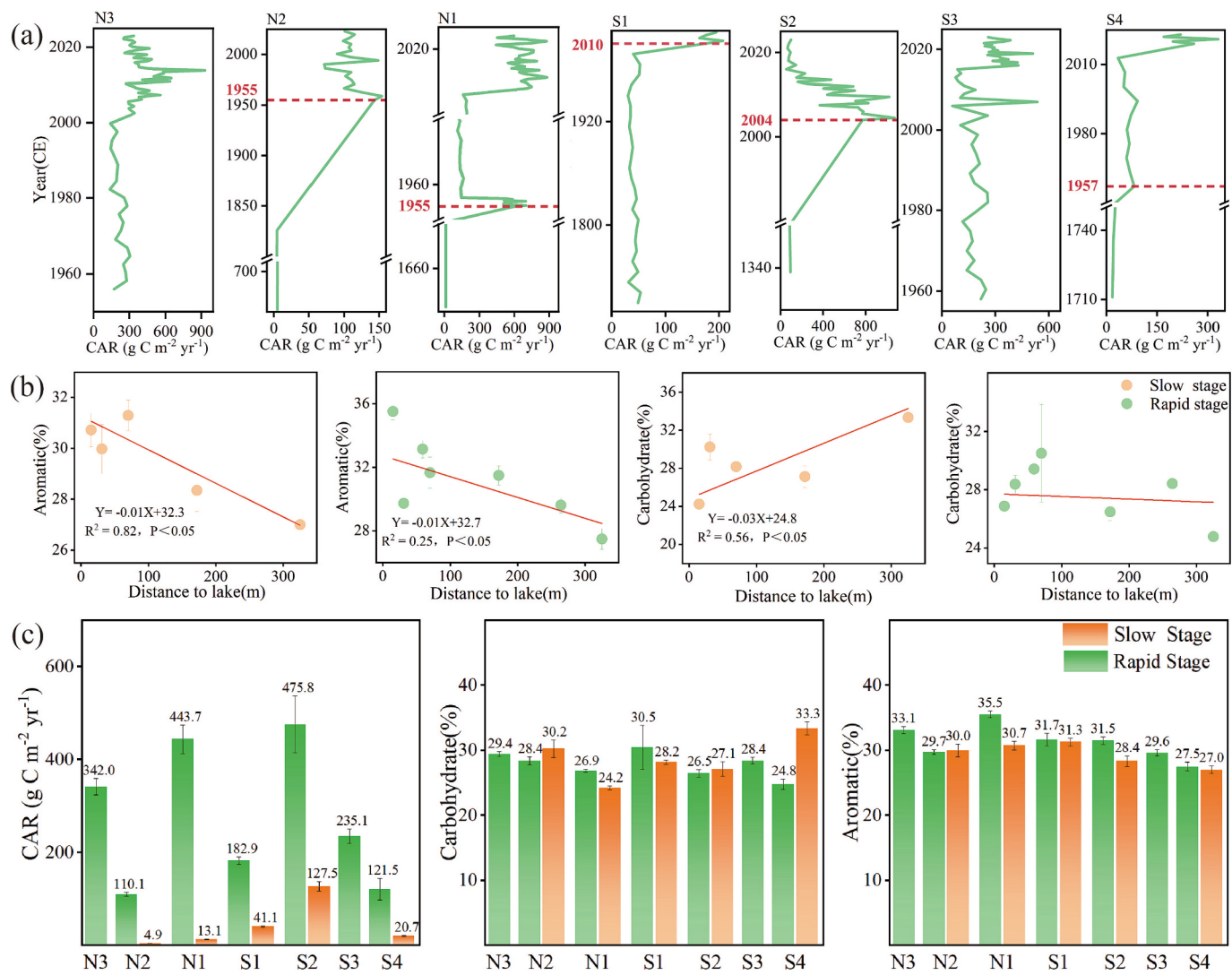


Fig. 4. (a) the carbon accumulation rates (CARs) in both transects. The dashed line represents the boundary between the “Rapid accumulation stage” and the “Slow accumulation stage”, (b) correlation analysis between organic compounds and distance, (c) the average carbon accumulation rates (CARs) and organic compounds in all cores.

occurs in two stages with the infilling process of peatlands (Fig. 4a). However, cores N3 and S3 did not show the expected low CARs values, which may be due to the collapse of permafrost, potentially preventing the sampling of the corresponding peat layers. The differences in peat accumulation between stages are influenced by a combination of factors, such as climate warming, water table fluctuations, and plant types (Ruppel et al., 2013; Xing et al., 2015; Magnan et al., 2022). Pioneering hydrophytic plants colonize in nutrient-rich sediments (Ruppel et al., 2013), the waterlogging conditions limit the decomposition of plant remains, leading to a noticeable carbon accumulation rates (Glaser et al., 2004; Loisel and Garneau, 2010). Loisel and Garneau (2010) reported that the CARs of peatlands (Northern Québec, Canada) ranged from 9.1 to 41.7 g C m⁻² yr⁻¹ with higher water table, which is similar to the CARs observed during the “Slow accumulation stage” in this study. This may be due to intermittent fluctuations in water table and the short growing seasons of hydrophytic plants with non-woody stems, the CARs remained low values throughout “Slow accumulation stage”. However, although peat begin accumulated in this stage, the high water table and hydrophytic plants associated with younger peatland have a warming effect by increasing CH₄ emissions (Juutinen et al., 2013; Swindles et al., 2015; Juselius-Rajamäki et al., 2025).

Meteorological data show that extreme droughts and high

temperatures in the study area over the past 120 years were primarily concentrated between 1920 and 1954 CE (Peng, 2019; Peng, 2020) (Fig. 5e-f). The frequent occurrences of extreme drought and extreme high temperatures are prone to trigger drought events, which accelerate the decline of lake water table and surrounding peatlands (e.g. Klein et al., 2013). The hydrophytic plants further transition to dry-adapted *Sphagnum* and shrubs (Olefeldt et al., 2021; Errington et al., 2024), as observed in the field at thermokarst lake margins: plants gradient from sedges to *Ericaceae* shrubs, *Sphagnum*, and *Betulaceae*. Meanwhile, the increase in temperature promotes photosynthesis and extends the growing season in mid-high latitude ecosystems, which increases the net primary productivity (NPP) of plants (Breeuwer et al., 2009; Ireland et al., 2013; Magnan et al., 2022), thereby facilitating the peat carbon rapid accumulation (Gallego-Sala et al., 2018; Morris et al., 2018). Although some studies suggest that warming may also increase the peat decomposition rate (Dorrepael et al., 2009; Klein et al., 2013), the positive effect of extended growing seasons and increased NPP outweighs the decomposition effect (Beilman et al., 2009; Xing et al., 2015; Hugelius et al., 2020). Consequently, frequent extreme drought events and hydrological fluctuations led to a shift in the CARs, marking the beginning of the “Rapid accumulation stage” around 1950s (Fig. 4a).

We estimate that the increments of organic carbon stock was 11,400 t

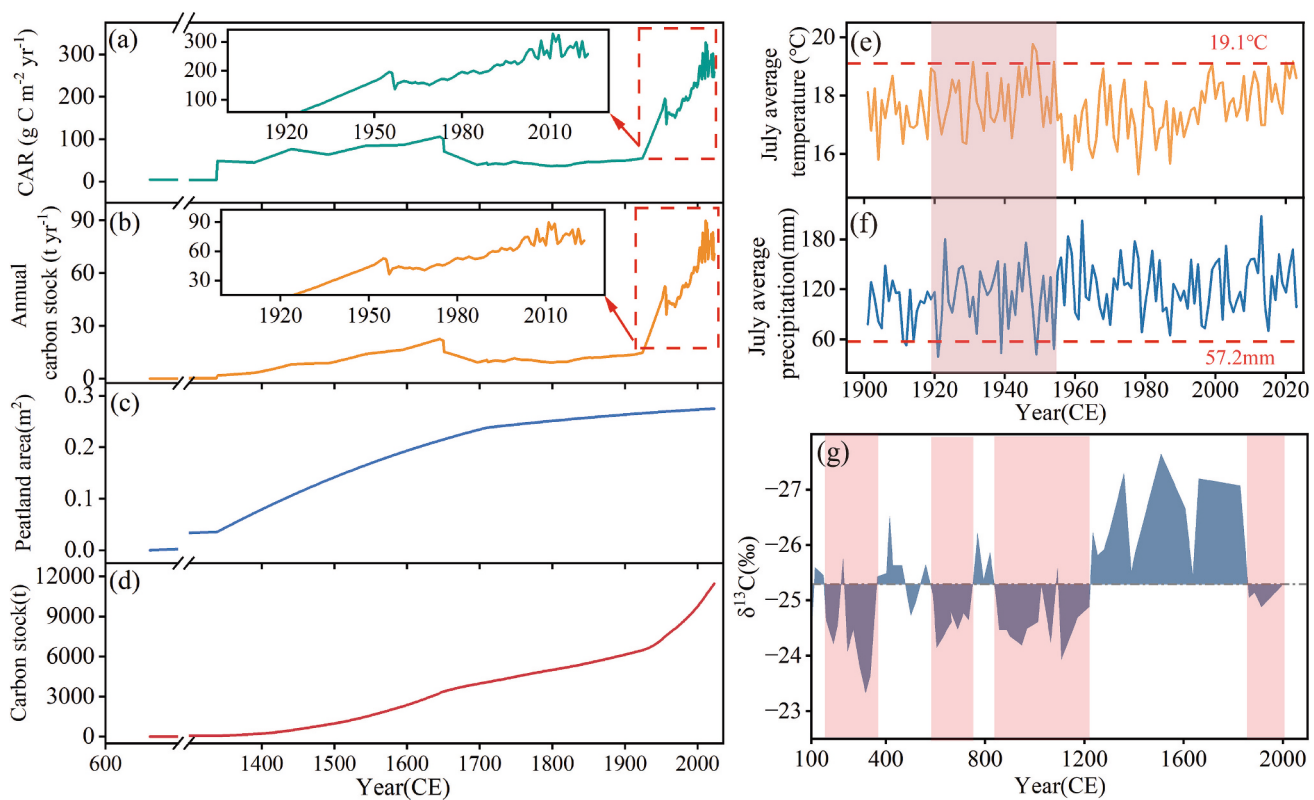


Fig. 5. Carbon stock dynamic: (a) annual average CARs, (b) annual carbon stock increments, (c) total area of peatlands lateral expansion, (d) total carbon stock, (e-f) the precipitation corresponding to the 5th percentile (≤ 57.2 mm) and the temperature at the 95th percentile (≥ 19.1 °C) over the past century are defined as thresholds for extreme drought and extreme heat events, respectively. (g) significant drought events during 50–400 CE, 600–750 CE and 820–1200 CE based on the carbon isotope composition ($\delta^{13}\text{C}$) of C3 plants (Hong et al., 2001).

(Fig. 5d), approximately $39.57 \text{ kg C m}^{-2}$, which is close to previous studies of the peatlands carbon stock in the Greater Khingan Mountains with $51.48 \text{ kg C m}^{-2}$ (Xing et al., 2015). The sharp increase in carbon stock during the “Rapid accumulation stage” since 1955 CE, accounting for 35 %. Notably, the average CARs at thermokarst lake margins reached $258.2 \text{ g C m}^{-2} \text{ yr}^{-1}$ in the rapid accumulation stage, significantly higher than the long-term average carbon accumulation rates of peatlands in Northeast China, ranges from 5.74 to $129.31 \text{ g C m}^{-2} \text{ yr}^{-1}$ (Xing et al., 2015). We boldly estimate that 50–100 years later, the average carbon stock of the newly expanded peatlands might surpass the overall average carbon stock of the region, which might cause uncertainty in estimating the total carbon stock of peatlands. Although our result show that the deeply buried peat layer also has a relatively high OM after undergoing decomposition for hundreds or even thousands of years, we cannot exclude the possibility that the higher CARs observed in this study are due to the incomplete decomposition of younger plant remains (Young et al., 2021). Some of the rapidly accumulating peat layers may not become long-term peatland carbon sinks, especially when the burial conditions are unstable, this should be viewed with considerable circumspection.

4.3. Stability of carbon pool

Carbohydrate contents were lower in the deeper peat layer and with an increase observed as the distance from core sites to the lakeshore. This is likely due to lake water with abundant hydrophytic plants and typically has higher nutrients levels compared to ombrotrophic peatlands (Fuchs et al., 2019). Sufficient nitrogen availability supports the synthesis of proteins, enzymes, and nucleic acids by soil microbes, thereby enhancing microbial abundance (Geisseler et al., 2010), and promotes the decomposition of organic matter. However, under

waterlogged and anaerobic conditions, oxidative reactions are limited, reducing the decomposition rate of organic compounds (Juselius-Rajamäki et al., 2023; Yeloff and Mauquoy, 2006). As a result, less stable compounds, such as carbohydrates, are more easily decomposed than other organic materials (Liu et al., 2019), resulting in a lower proportion of carbohydrate contents in the proximal peat of thermokarst lake and lower peat layer. In contrast, organic matter in the more distal peatlands, further from modern thermokarst lakes, has undergone longer periods of decomposition, leading to a noticeable decrease in the more stable aromatic compounds in the peat as the distance from the lakeshore increases ($R^2 = 0.82$, $R^2 = 0.25$) (Fig. 4b). However, net primary productivity (NPP) in the peatlands at thermokarst lake margins increased, contributing to an increased input of plant remains into the peatlands, which raises the baseline of carbohydrate content. As a result, the proportion of carbohydrate compounds increases with the distance from the peatlands to the lakeshore ($R^2 = 0.56$) (Fig. 4b).

Moreover, as CARs entered the “Rapid accumulation stage”, the aromatic compounds in peat of all cores are significantly higher than in the “Slow accumulation stage”. We observed that aromatic contents in surface peat layers of core N3 (shrub and *Sphagnum*-dominated) were significantly higher than in cores N2 and N1 (sedge-dominated) ($P < 0.05$), and the aromatic contents in surface peat layers of cores S2 and S3 (shrub and *Sphagnum*-dominated) were higher than in core S1 (sedge-dominated) (Fig. 4c). Our results suggest that as the surface level of the peatlands rises, the plants shift from minerotrophic species (e.g. *Carex lasiocarpa* and *Phragmites australis*) to ombrotrophic species (e.g. *Sphagnum* and shrubs) (Camill, 1999; Olefeldt et al., 2021), leading to the increase in aromatic compounds with higher stability in peatland (Cong et al., 2020). This also supports the notion that *Sphagnum* and shrubs, with their higher aromatic content, exhibit greater decay resistance and contribute to enhanced carbon accumulation (e.g. Loisel and

Yu, 2013; Juselius-Rajamäki, 2025; Zhang et al., 2025). Therefore, with the peatlands areal increase and the rapid accumulation of organic carbon, the carbon pool in peatlands at thermokarst lake margins may become more stable, this could also be one of the reasons for the higher CARs.

5. Conclusions

This study provides new insights into the infilling process of peatlands and the evolution of carbon pool stability. The results demonstrate a strong correlation between climate change and peatland dynamics at thermokarst lake margins in the Greater Khingan Mountains. Several drought events in Northeast China, which promoted peatlands lakeward expansion with rates ranging from 2 cm yr^{-1} to 32 cm yr^{-1} . Strongly influenced by hydrological fluctuations and warming, the carbon accumulation of the studied peatlands commenced with a stage of slow accumulation, and then entered a rapid accumulation stage after the 1950s, with the carbon accumulation rates increasing from $45.2 \pm 5.5 \text{ g C m}^{-2} \text{ yr}^{-1}$ to $330.5 \pm 14.4 \text{ g C m}^{-2} \text{ yr}^{-1}$. Additionally, the aromatic compounds increased with plant changes caused by the water table decreasing, the stability of carbon pool seemed to accelerate the peat accumulation enters rapid accumulation stage.

CRediT authorship contribution statement

Jiangtao Gao: Writing – review & editing, Writing – original draft, Investigation, Conceptualization. **Jinxin Cong:** Writing – review & editing, Investigation. **Guangxin Li:** Writing – review & editing, Investigation. **Yingjie Shi:** Writing – review & editing. **Dongxue Han:** Writing – review & editing, Investigation, Funding acquisition. **Guoping Wang:** Writing – review & editing, Investigation. **Chuanyu Gao:** Writing – review & editing, Funding acquisition, Conceptualization.

Declaration of competing interest

The authors declare that they have no known competing financial interests or personal relationships that could have appeared to influence the work reported in this paper.

Acknowledgments

The authors gratefully acknowledge the assistance of the Analysis and Test Center of the Northeast Institute of Geography and Agroecology (IGA) of the Chinese Academy of Sciences (CAS). This work was supported by the National Natural Science Foundation of China (Grant Nos. 42494822, 42301120, 42171103, 42330509), the National Key Research and Development Program of China (2023YFF0807201), and the Jilin Provincial Science and Technology Department (20250101022JJ).

Appendix A. Supplementary data

Supplementary data to this article can be found online at <https://doi.org/10.1016/j.palaeo.2025.113281>.

Data availability

The Meteorological data used in this study are available from the National Tibetan Plateau/Third Pole Environment Data Center at <https://doi.org/10.11888/Meteoro.tpd.270961> and <https://doi.org/10.5281/zenodo.3114194> (Peng, 2019; Peng, 2020). Data of peat cores in this paper are available through Mendeley Data at <https://doi.org/10.17632/xn5845d4xy.1>.

References

- Beilman, D.W., MacDonald, G.M., Smith, L.C., Reimer, P.J., 2009. Carbon accumulation in peatlands of West Siberia over the last 2000 years. *Glob. Biogeochem. Cycles* 23, 1–12. <https://doi.org/10.1029/2007GB003112>.
- Breeuwer, A., Robroek, B.J.M., Limpens, J., Heijmans, M.M.P.D., Schouten, M.G.C., Berendse, F., 2009. Decreased summer water table depth affects peatland vegetation. *Basic Appl. Ecol.* 10, 330–339. <https://doi.org/10.1016/j.baee.2008.05.005>.
- Camill, P., 1999. Patterns of boreal permafrost peatland vegetation across environmental gradients sensitive to climate warming. *Can. J. Bot.* 77, 721–733. <https://doi.org/10.1139/b99-008>.
- Campbell, D.R., Duthie, H.C., Warner, B.G., 1997. Post-glacial development of a kettle-hole peatland in southern Ontario. *Ecoscience* 4, 404–418. <https://doi.org/10.1080/11956860.1997.11682419>.
- Chai, X., 1990. Peat Geo-Science. Geological Publishing House, Beijing (in Chinese).
- Cong, J., Gao, C., Han, D., Li, Y., Wang, G., 2020. Stability of the permafrost peatlands carbon pool under climate change and wildfires during the last 150 years in the northern Great Khingan Mountains, China. *Sci. Total Environ.* 712, 136476. <https://doi.org/10.1016/j.scitotenv.2019.136476>.
- Dorrepaal, E., Toet, S., van Logtestijn, R.S.P., Swart, E., van de Weg, M.J., Callaghan, T.V., Aerts, R., 2009. Carbon respiration from subsurface peat accelerated by climate warming in the subarctic. *Nature* 460, 616–U679. <https://doi.org/10.1038/nature08216>.
- Errington, R.C., Macdonald, S.E., Bhatti, J.S., 2024. Rate of permafrost thaw and associated plant community dynamics in peatlands of northwestern Canada. *J. Ecol.* 112, 1565–1582. <https://doi.org/10.1111/1365-2745.14339>.
- Fewster, R.E., Swindles, G.T., Carrivick, J.L., Galka, M., Roland, T.P., McKeown, M., Sutherland, J.L., Tweed, F., Mullan, D., Graham, C., Gallego-Sala, A., Morris, P.J., 2025. Climate Warming and Deglaciation Drive New Peat Formation in the Southern Alps, Aotearoa/New Zealand. *Geophys. Res. Lett.* 52, e2024GL113786. <https://doi.org/10.1029/2024GL113786>.
- Fuchs, M., Lenz, J., Jock, S., Nitze, I., Jones, B.M., Strauss, J., Gunther, F., Grosse, G., 2019. Organic Carbon and Nitrogen stocks along a Thermokarst Lake Sequence in Arctic Alaska. *J. Geophys. Res. Biogeosci.* 124, 1230–1247. <https://doi.org/10.1029/2018JG004591>.
- Gallego-Sala, A.V., Charman, D.J., Brewer, S., Page, S.E., Prentice, I.C., Friedlingstein, P., Moreton, S., Amesbury, M.J., Beilman, D.W., Björck, S., Blyakharchuk, T., Bochicchio, C., Booth, R.K., Bunbury, J., Camill, P., Carless, D., Chimmner, R.A., Clifford, M., Cressey, E., Courtney-Mustaphi, C., De Vleeschouwer, F., de Jong, R., Fialkiewicz-Koziel, B., Finkelstein, S.A., Garneau, M., Githumbi, E., Hribjlan, J., Holmquist, J., Hughes, P.D.M., Jones, C., Jones, M.C., Karofeld, E., Klein, E.S., Kokfelt, U., Korhola, A., Lacourte, T., Le Roux, G., Lamentowicz, M., Large, D., Lavoie, M., Loisel, J., Mackay, H., MacDonald, G.M., Makila, M., Magnan, G., Marchant, R., Marcisz, K., Cortizas, A.M., Massa, C., Mathijssen, P., Mauquoy, D., Mighall, T., Mitchell, F.J.G., Moss, P., Nichols, J., Oksanen, P.O., Orme, L., Packalen, M.S., Robinson, S., Roland, T.P., Sanderson, N.K., Sannel, A.B.K., Silva-Sánchez, N., Steinberg, N., Swindles, G.T., Turner, T.E., Uglow, J., Välijärvi, M., van Bellen, S., van der Linden, M., van Geel, B., Wang, G.P., Yu, Z.C., Zaragoza-Castells, J., Zhao, Y., 2018. Latitudinal limits to the predicted increase of the peatland carbon sink with warming. *Nat. Clim. Chang.* 8, 907. <https://doi.org/10.1038/s41558-018-0271-1>.
- Geisseler, D., Horwath, W.R., Joergensen, R.G., Ludwig, B., 2010. Pathways of nitrogen utilization by soil microorganisms—a review. *Soil Biol. Biochem.* 42, 2058–2067. <https://doi.org/10.1016/j.soilbio.2010.08.021>.
- Glaser, P.H., Hansen, B.C.S., Siegel, D.I., Reeve, A.S., Morin, P.J., 2004. Rates, pathways and drivers for peatland development in the Hudson Bay Lowlands, northern Ontario, Canada. *J. Ecol.* 92, 1036–1053. <https://doi.org/10.1111/j.0022-0477.2004.00931.x>.
- Gorham, E., 1991. Northern Peatlands: Role in the Carbon Cycle and Probable responses to Climatic Warming. *Ecol. Appl.* 1, 182–195. <https://doi.org/10.2307/1941811>.
- Han, D.X., Gao, C.Y., Yu, Z.C., Yu, X.F., Li, Y.H., Cong, J.X., Wang, G.P., 2019. Late Holocene vegetation and climate changes in the Great Hinggan Mountains, Northeast China. *Quat. Int.* 532, 138–145. <https://doi.org/10.1016/j.quaint.2019.11.017>.
- Harris, L.I., Olefeldt, D., Pelletier, N., Blodau, C., Knorr, K.H., Talbot, J., Heffernan, L., Turetsky, M., 2023. Permafrost thaw causes large carbon loss in boreal peatlands while changes to peat quality are limited. *Glob. Chang. Biol.* 29, 5720–5735. <https://doi.org/10.1111/gcb.16894>.
- Heffernan, L., Estop-Aragonés, C., Knorr, K.H., Talbot, J., Olefeldt, D., 2020. Long-term impacts of permafrost thaw on carbon storage in peatlands: deep losses offset by surficial accumulation. *J. Geophys. Res. Biogeosci.* 125, e2019JG005501. <https://doi.org/10.1029/2019JG005501>.
- Hodgkins, S.B., Richardson, C.J., Dommain, R., Wang, H., Glaser, P.H., Verbeke, B., Winkler, B.R., Cobb, A.R., Rich, V.I., Missilmani, M., Flanagan, N., Ho, M., Hoyt, A.M., Harvey, C.F., Vining, S.R., Hough, M.A., Moore, T.R., Richard, P.J.H., De La Cruz, F.B., Toufaily, J., Hamdan, R., Cooper, W.T., Chanton, J.P., 2018. Tropical peatland carbon storage linked to global latitudinal trends in peat recalcitrance. *Nat. Commun.* 9, 3640. <https://doi.org/10.1038/s41467-018-06050-2>.
- Hong, Y., Wang, Z., Jiang, H., Lin, Q., Hong, B., Zhu, Y., Wang, Y., Xu, L., Leng, X., Li, H., 2001. A 6000-year record of changes in drought and precipitation in north eastern China based on a $\delta^{13}\text{C}$ time series from peat cellulose. *Earth Planet. Sci. Lett.* 185, 111–119. [https://doi.org/10.1016/S0012-821X\(00\)00367-8](https://doi.org/10.1016/S0012-821X(00)00367-8).
- Hugelius, G., Loisel, J., Chadburn, S., Jackson, R.B., Jones, M., MacDonald, G., Marushchak, M., Olefeldt, D., Packalen, M., Siewert, M.B., Treat, C., Turetsky, M., Voigt, C., Yu, Z.C., 2020. Large stocks of peatland carbon and nitrogen are

- vulnerable to permafrost thaw. *PNAS* 117, 20438–20446. <https://doi.org/10.1073/pnas.1916387117>.
- Hutchings, J.A., Bianchi, T.S., Kaufman, D.S., Kholodov, A.L., Vaughn, D.R., Schuur, E.A.G., 2019. Millennial-scale carbon accumulation and molecular transformation in a permafrost core from Interior Alaska. *Geochim. Cosmochim. Acta* 253, 231–248. <https://doi.org/10.1016/j.gca.2019.03.028>.
- Ireland, A.W., Booth, R.K., Hotchkiss, S.C., Schmitz, J.E., 2013. A comparative study of within-basin and regional peatland development: implications for peatland carbon dynamics. *Quat. Sci. Rev.* 61, 85–95. <https://doi.org/10.1016/j.quascirev.2012.10.035>.
- Juselius-Rajamäki, T., 2025. The Ongoing Expansion of the Northern Peatlands: Peat Formation, Succession, and Driving Factors in the Peatland Frontiers.
- Juselius-Rajamäki, T., Välijanta, M., Korhola, A., Korhola, A., 2023. The ongoing lateral expansion of peatlands in Finland. *Glob. Chang. Biol.* 29, 7173–7191. <https://doi.org/10.1111/gcb.16988>.
- Juselius-Rajamäki, T., Piilo, S., Salminen-Paatero, S., Tuomaala, E., Virtanen, T., Korhola, A., Autio, A., Marttila, H., Ala-Aho, P., Lohila, A., Välijanta, M., 2025. External and internal drivers behind the formation, vegetation succession, and carbon balance of a subarctic fen margin. *Biogeosciences* 22, 3047–3071. <https://doi.org/10.5194/bg-22-3047-2025>.
- Juutinen, S., Välijanta, M., Kuutti, V., Laine, A.M., Virtanen, T., Seppä, H., Weckström, J., Tuittila, E.S., 2013. Short-term and long-term carbon dynamics in a northern peatland stream-lake continuum: a catchment approach. *J. Geophys. Res. Biogeosci.* 118 (1), 171–183. <https://doi.org/10.1002/jgrc.20028>.
- Klein, E.S., Yu, Z., Booth, R.K., 2013. Recent increase in peatland carbon accumulation in a thermokarst lake basin in southwestern Alaska. *Palaeogeogr. Palaeoclimatol. Palaeoecol.* 392, 186–195. <https://doi.org/10.1016/j.palaeo.2013.09.009>.
- Kratz, T.K., Dewitt, C.B., 1986. Internal Factors Controlling Peatland-Lake Ecosystem Development. *Ecology* 67, 100–107. <https://doi.org/10.2307/1938507>.
- Liu, J., Gao, G., Jie, D., Qiu, S., Ren, G., Tang, J., Qin, X., 2007. The Natural Environment and the Influence of Human Activity Research in Northeast China. Science Press, Beijing (in Chinese).
- Liu, L.F., Chen, H., Jiang, L., Zhan, W., Hu, J., He, Y.X., Liu, J.L., Xue, D., Zhu, D., Zhao, C., Yang, G., 2019. Response of anaerobic mineralization of different depths peat carbon to warming on Zoige plateau. *Geoderma* 337, 1218–1226. <https://doi.org/10.1016/j.geoderma.2018.10.031>.
- Loisel, J., Garneau, M., 2010. Late Holocene paleoecohydrology and carbon accumulation estimates from two boreal peat bogs in eastern Canada: potential and limits of multi-proxy archives. *Palaeogeogr. Palaeoclimatol. Palaeoecol.* 291, 493–533. <https://doi.org/10.1016/j.palaeo.2010.03.020>.
- Loisel, J., Yu, Z., 2013. Recent acceleration of carbon accumulation in a boreal peatland, south Central Alaska. *J. Geophys. Res. Biogeosci.* 118, 41–53. <https://doi.org/10.1029/2012JG001978>.
- Magnan, G., Sanderson, N.K., Piilo, S., Pratte, S., Välijanta, M., van Bellen, S., Zhang, H., Garneau, M., 2022. Widespread recent ecosystem state shifts in high-latitude peatlands of northeastern Canada and implications for carbon sequestration. *Glob. Chang. Biol.* 28 (5), 1919–1934. <https://doi.org/10.1111/gcb.16032>.
- Morris, P.J., Swindles, G.T., Valdes, P.J., Ivanovic, R.F., Gregoire, L.J., Smith, M.W., Tarasov, L., Haywood, A.M., Bacon, K.L., 2018. Global peatland initiation driven by regionally asynchronous warming. *Proc. Natl. Acad. Sci.* 115, 4851–4856. <https://doi.org/10.1073/pnas.1717838115>.
- Morris, P.J., Davies, M.L., Baird, A.J., Balliston, N., Bourgault, M.A., Clymo, R.S., Fewster, R.E., Furukawa, A.K., Holden, J., Kessel, E., Ketcheson, S.J., Kloke, B., Larocque, M., Marttila, H., Menberu, M.W., Moore, P.A., Price, J.S., Ronkanen, A.K., Rosa, E., Strack, M., Surridge, B.W.J., Waddington, J.M., Whittington, P., Wilkinson, S.L., 2022. Saturated hydraulic conductivity in Northern peats inferred from other measurements. *Water Resour. Res.* 58, e2022WR033181. <https://doi.org/10.1029/2022WR033181>.
- Olefeldt, D., Goswami, S., Grossje, G., Hayes, D., Hugelius, G., Kuhry, P., McGuire, C.E., Romanovsky, V.E., Sannel, A.B., Schuur, E.A., Turetsky, M.R., 2016. Circumpolar distribution and carbon storage of thermokarst landscapes. *Nat. Commun.* 7, 13043. <https://doi.org/10.1038/ncomms13043>.
- Olefeldt, D., Heffernan, L., Jones, M.C., Sannel, A.B.K., Treat, C.C., Turetsky, M.R., 2021. Permafrost thaw in northern peatlands: rapid changes in ecosystem and landscape functions. *Ecosyst. Collaps. Clim. Chang.* 27–67.
- Olid, C., Binder, R., Nilsson, M.B., Eriksson, T., Klaminder, J., 2017. Effects of warming and increased nitrogen and sulfur deposition on boreal mire geochemistry. *Appl. Geochem.* 78, 149–157. <https://doi.org/10.1016/j.apgeochem.2016.12.015>.
- Page, S.E., Baird, A.J., 2016. Peatlands and Global Change: Response and Resilience. *Annu. Rev. Environ. Resour.* 41 (41), 35–57. <https://doi.org/10.1146/annurev-environ-110615-085520>.
- Payette, S., Delwaide, A., Caccianiga, M., Beauchemin, M., 2004. Accelerated thawing of subarctic peatland permafrost over the last 50 years. *Geophys. Res. Lett.* 31 (18). <https://doi.org/10.1029/2004GL020358>.
- Peng, S., 2019. 1-km monthly mean temperature dataset for China (1901–2023). In: National Tibetan Plateau/Third Pole Environment Data Center. <https://doi.org/10.11888/Meteoro.tpdc.270961>.
- Peng, S., 2020. 1-km monthly precipitation dataset for China (1901–2023). In: National Tibetan Plateau/Third Pole Environment Data Center. <https://doi.org/10.5281/zenodo.3114194>.
- Reimer, P.J., Austin, W.E.N., Bard, E., Bayliss, A., Blackwell, P.G., Bronk Ramsey, C., Butzin, M., Cheng, H., Edwards, R.L., Friedrich, M., Grootes, P.M., Guilderson, T.P., Hajdas, I., Heaton, T.J., Hogg, A.G., Hughen, K.A., Kromer, B., Manning, S.W., Muscheler, R., Palmer, J.G., Pearson, C., van der Plicht, J., Reimer, R.W., Richards, D.A., Scott, E.M., Southon, J.R., Turney, C.S.M., Wacker, L., Adolphi, F.,
- Büntgen, U., Capano, M., Fahrni, S.M., Fogtmann-Schulz, A., Friedrich, R., Köhler, P., Kudsk, S., Miyake, F., Olsen, J., Reinig, F., Sakamoto, M., Sookdeo, A., Talamo, S., 2020. The IntCal20 Northern Hemisphere radiocarbon age calibration curve (0–55 cal kBP). *Radiocarbon* 62, 725–757. <https://doi.org/10.1017/RDC.2020.41>.
- Roulet, N.T., Lafleur, P.M., Richard, P.J.H., Moore, T.R., Humphreys, E.R., Bubier, J., 2007. Contemporary carbon balance and late Holocene carbon accumulation in a northern peatland. *Glob. Chang. Biol.* 13, 397–411. <https://doi.org/10.1111/j.1365-2486.2006.01292.x>.
- Ruppel, M., Välijanta, M., Virtanen, T., Korhola, A., 2013. Postglacial spatiotemporal peatland initiation and lateral expansion dynamics in North America and northern Europe. *Holocene* 23, 1596–1606. <https://doi.org/10.1177/0959683613499053>.
- Salinger, M., 2005. Climate variability and change: past, present and future – an overview. *Clim. Chang.* 70, 9–29. <https://doi.org/10.1007/s10584-005-5936-x>.
- Sannel, A.B.K., Kuhry, P., 2011. Warming-induced destabilization of peat plateau/thermokarst lake complexes. *J. Geophys. Res. Biogeosci.* 116, G03035. <https://doi.org/10.1029/2010JG001635>.
- Schuur, E.A.G., McGuire, A.D., Schädel, C., Grosse, G., Harden, J.W., Hayes, D.J., Hugelius, G., Koven, C.D., Kuhry, P., Lawrence, D.M., Natali, S.M., Olefeldt, D., Romanovsky, V.E., Schaefer, K., Turetsky, M.R., Treat, C.C., Vonk, J.E., 2015. Climate change and the permafrost carbon feedback. *Nature* 520, 171–179. <https://doi.org/10.1038/nature14338>.
- Shaposhnikova, M., Duguay, C., Roy-Leveillee, P., 2023. Bedfast and floating-ice dynamics of thermokarst lake using a temporal deep-learning mapping approach: case study of the Old Crow Flats, Yukon, Canada. *Cryosphere* 17, 1697–1721. <https://doi.org/10.5194/tc-17-1697-2023>.
- Silvestri, S., Christensen, C.W., Lysdahl, A.O.K., Anschütz, H., Pfaffhuber, A.A., Vizzoli, A., 2019. Peatland volume mapping over resistive substrates with airborne electromagnetic technology. *Geophys. Res. Lett.* 46, 6459–6468. <https://doi.org/10.1029/2019GL083025>.
- Strack, M., 2008. Peatlands and Climate Change. International Peat Society, IPS.
- Swindles, G.T., Morris, P.J., Mullan, D., Watson, E.J., Turner, T.E., Roland, T.P., Amesbury, M.J., Kokfelt, U., Schoning, K., Pratte, S., Gallego-Sala, A., Charman, D.J., Sanderson, N., Garneau, M., Carrivick, J.L., Woults, C., Holden, J., Parry, L., Galloway, J.M., 2015. The long-term fate of permafrost peatlands under rapid climate warming. *Sci. Rep.* 5, 1–6. <https://doi.org/10.1038/srep17951>.
- Tarnocai, C., Canadell, J.G., Schuur, E.A.G., Kuhry, P., Mazhitova, G., Zimov, S., 2009. Soil organic carbon pools in the northern circumpolar permafrost region. *Glob. Biogeochem. Cycles* 23. <https://doi.org/10.1029/2008gb003327>.
- Temmink, R.J.M., Lamers, L.P.M., Angelini, C., Bouma, T.J., Fritz, C., van de Koppel, J., Lexmond, R., Rietkerk, M., Silliman, B.R., Joosten, H., van der Heide, T., 2022. Recovering wetland biogeomorphic feedbacks to restore the world's biotic carbon hotspots. *Science* 376, eabn1479. <https://doi.org/10.1126/science.abn1479>.
- Tolonen, K., Turunen, J., 1996. Accumulation rates of carbon in mires in Finland and implications for climate change. *Holocene* 6, 171–178. <https://doi.org/10.1177/095968369600600204>.
- Vonk, J.E., Tank, S.E., Bowden, W.B., Laurion, I., Vincent, W.F., Alekseychik, P., Amyot, M., Billett, M.F., Canário, J., Cory, R.M., Deshpande, B.N., Helbig, M., Jammet, M., Karlsson, J., Larouche, J., MacMillan, G., Rautio, M., Anthony, K.M.W., Wicklund, K.P., 2015. Reviews and syntheses: Effects of permafrost thaw on Arctic aquatic ecosystems. *Biogeosciences* 12, 7129–7167. <https://doi.org/10.5194/bg-12-7129-2015>.
- Williams, J.W., Shuman, B., Bartlein, P.J., Diffenbaugh, N.S., Webb, T., 2010. Rapid, time-transgressive, and variable responses to early Holocene midcontinental drying in North America. *Geology* 38. <https://doi.org/10.1130/G30413.1>, 135e138.
- Xing, W., Bao, K.S., Gallego-Sala, A.V., Charman, D.J., Zhang, Z.Q., Gao, C.Y., Lu, X.G., Wang, G.P., 2015. Climate controls on carbon accumulation in peatlands of Northeast China. *Quat. Sci. Rev.* 115, 78–88. <https://doi.org/10.1016/j.quascirev.2015.03.005>.
- Yao, L., Gong, Y., Ye, C., Shi, W., Zhang, K., Du, M., Zhang, Q., 2022. Soil denitrification rates are more sensitive to hydrological change than restoration approaches in a unique riparian zone. *Functional Ecology* 36 (8), 2056–2068. <https://doi.org/10.1016/j.scitotenv.2020.142924>.
- Yeloff, D., Mauquoy, D., 2006. The influence of vegetation composition on peat humification: implications for palaeoclimatic studies. *Boreas* 35, 662–673. <https://doi.org/10.1080/0300948060690860>.
- Young, D.M., Baird, A.J., Gallego-Sala, A.V., Loisel, J., 2021. A cautionary tale about using the apparent carbon accumulation rate (aCAR) obtained from peat cores. *Sci. Rep.* 11, 9547. <https://doi.org/10.1038/s41598-021-88766-8>.
- Yu, Z.C., 2011. Holocene carbon flux histories of the world's peatlands: Global carbon-cycle implications. *Holocene* 21, 761–774. <https://doi.org/10.1177/0959683610386982>.
- Yu, Z.C., Loisel, J., Brosseau, D.P., Beilman, D.W., Hunt, S.J., 2010. Global peatland dynamics since the last Glacial Maximum. *Geophys. Res. Lett.* 37, 13.
- Zhang, M.M., Bu, Z.J., Jiang, M., Wang, S.Z., Liu, S.S., Jin, Q., Shi, P.H., 2019. Mid-late Holocene maar lake-mire transition in Northeast China triggered by hydroclimatic variability. *Quat. Sci. Rev.* 220, 215–229. <https://doi.org/10.1016/j.quascirev.2019.07.027>.
- Zhang, Y.M., Huang, X.Y., Zhao, B.Y., Yan, C.Y., Zhao, H.Y., Zhang, H.B., Halama, T.A., Peel, R.H., Vreeken, M., Gallego-Sala, A.V., Pancost, R.D., Xie, S.C., 2025. Microbial responses to changing plant community protect peatland carbon stores during Holocene drying. *Nat. Commun.* 16, 6912. <https://doi.org/10.1038/s41467-025-62175-1>.
- Zhou, Y.W., Guo, D.X., Qiu, G., Cheng, G.D., Li, S.D., 2000. China Permafrost. Science Press, Beijing.